JACS
JOURNAL OF THE AMERICAN CHEMICAL SOCIETY
Article
pubs.acs.org/JACS

Spontaneous Prebiotic Formation of a β-Ribofuranoside That Self-Assembles with a Complementary Heterocycle

Michael C. Chen,[‡,†] Brian J. Cafferty,[‡,†] Irena Mamajanov,[†] Isaac Gállego,[†] Jaheda Khanam,[†] Ramanarayanan Krishnamurthy,[§] and Nicholas V. Hud*[,†]

[†]School of Chemistry and Biochemistry and Parker H. Petit Institute for Bioengineering and Bioscience, Georgia Institute of Technology, Atlanta, Georgia 30332, United States

[§]Department of Chemistry, The Scripps Research Institute, La Jolla, California 92037, United States

Supporting Information

ABSTRACT: The RNA World hypothesis is central to many current theories regarding the origin and early evolution of life. However, the formation of RNA by plausible prebiotic reactions remains problematic. Formidable challenges include glycosidic bond formation between ribose and the canonical nucleobases, as well as the inability of nucleosides to mutually select their pairing partners from a complex mixture of other molecules prior to polymerization. Here we report a one-pot model prebiotic reaction between a pyrimidine nucleobase (2,4,6-triaminopyrimidine, TAP) and ribose, which produces TAP-ribose conjugates in high yield (60−90%). When cyanuric acid (CA), a plausible ancestral nucleobase, is mixed with a crude TAP +ribose reaction mixture, micrometer-length supramolecular, noncovalent assemblies are formed. A major product of the TAP +ribose reaction is a β-ribofuranoside of TAP, which we term TARC. This nucleoside is also shown to efficiently form supramolecular assemblies in water by pairing and stacking with CA. These results provide a proof-of-concept system demonstrating that several challenges associated with the prebiotic emergence of RNA, or pre-RNA polymers, may not be as problematic as widely believed.

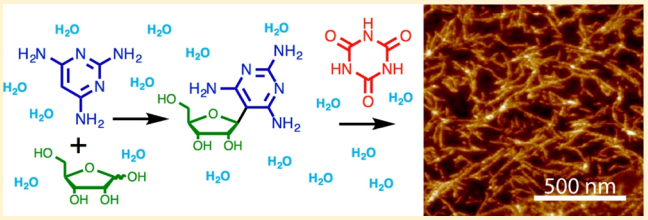

INTRODUCTION

Forty years ago, Orgel and co-workers explored abiotic nucleoside formation by drying and heating D-ribose with each of the four canonical nucleobases (adenine, guanine, cytosine, and uracil). Only adenine was found to form nucleosides in detectable amounts (~2% yield).[1−3] The poor glycosylation of the canonical nucleobases in model prebiotic reactions prompted the Orgel laboratory to explore the possibility that pyrimidine nucleosides were originally synthesized by nucleobase formation on a sugar scaffold,[4] a hypothesis for which a complete synthetic pathway was more recently demonstrated by Sutherland and co-workers through an elegant, albeit multistep, reaction.[5,6] Exploring the hypothesis that RNA evolved from a pre-RNA polymer,[7,8] Miller and co-workers,[9] and later our laboratory,[10] demonstrated that nucleosides are formed in good yields by reacting alternative heterocycles with ribose, specifically urazole and 2-pyrimidinone. The discovery of alternative heterocycles that readily undergo nucleoside formation suggests that alternative nucleosides could have been more abundant on the prebiotic earth than the canonical nucleosides.

Even if a prebiotic route to all four canonical nucleosides were established, the mechanism by which these nucleosides could have been selected from a complex mixture of molecules and coupled into RNA polymers without the aid of enzymes remains a daunting question. A major challenge arises due to the fact that the canonical mononucleotides and their free bases do not form Watson−Crick base pairs in water,[11,12] but rather associate by π-stacking. Thus, it is difficult to imagine how the four nucleobases of contemporary RNA would have been exclusively selected from among similar, but nonpairing, heterocycles for incorporation into the first informational polymers of life. We have proposed that this "paradox of base pairing"[13] could be overcome if there existed a set of recognition elements that are able to self-sort into noncovalent polymer assemblies prior to linkage by a common backbone.[14] Together, both prebiotic nucleoside formation and nucleobase selection may have not been so difficult if alternative heterocycles amenable to glycosylation and self-assembly formed the first informational polymers.

In search of alternative nucleobases that could form nucleosides robustly and make stable base pairs in water, we systematically considered all possible pyrimidines and purines with $-NH_2$, $=O$, or $-H$ as exocyclic groups. Of more than 80 possible candidates, 2,4,6-triaminopyrimidine (**TAP**) was one of the molecules chosen for investigation because its structure suggested the potential for enhanced reactivity with ribose,[15] and because **TAP** is well-known to form supramolecular assemblies with complementary heterocycles.[16−20] The H-bonding interactions between these heterocycles are similar to those found in Watson−Crick base pairs; however, their ability

Received: October 2, 2013
Published: December 13, 2013

   dx.doi.org/10.1021/ja410124v | J. Am. Chem. Soc. 2014, 136, 5640−5646

to interact along three "faces" enables the formation of larger structures (see below). Additionally, recent studies from our laboratory demonstrated the capability of modified, monomeric **TAP** to assemble with cyanuric acid (**CA**) in aqueous solution to form micrometer-length supramolecular assemblies.[20] Here we show that aqueous mixtures of **TAP** and ribose spontaneously form β-furanosyl nucleosides in high yields. Upon the addition of the complementary **CA**, the **TAP**−ribose conjugates assemble (within the unpurified reaction solution) to form micrometer-length noncovalent polymers consisting of thousands of ordered nucleosides.

RESULTS AND DISCUSSION

Drying and Mild Heating of TAP with Ribose Produces TAP−Ribose Conjugates. **TAP** and D-ribose were mixed together in water and heated under various conditions to assess the glycosylation potential of **TAP**. As shown in Figure 1, a considerable fraction of **TAP** becomes glycosylated to form **TAP**−ribose conjugates when the mixtures were dried at 35 °C (Figure 1). The reaction is robust, with **TAP**−ribose conjugates being produced in comparable yields when the ratio of **TAP** and ribose were varied over a factor of 5, and when the reaction was carried out at temperatures ranging from 35 to 95 °C (Figures S1−S5 Supporting Information [SI]). The yield of single-ribose **TAP** conjugates was maximized relative to double- and triple-ribose additions to **TAP** when mixtures were dried at the lower range of temperatures investigated and with **TAP**:ribose ratios close to unity. As shown in Figure 1B, HPLC analysis with simultaneous MS and UV absorption monitoring reveals that vacuum-assisted drying of a 1:2 **TAP**:ribose mixture at 35 °C for one day results in over 30% of **TAP** being modified by conjugation with ribose. Extended reaction times allowed maximum conversion of **TAP** to **TAP**−ribose conjugates. For example, the yield of single-ribose **TAP** conjugates (including nucleosides, see below) increased to around 60% after 10 days of drying at 35 °C, with momentary daily rehydration (which allowed the reaction to be carried out for multiple days under conditions of low water activity while remaining homogeneous) (Figure 1C). Reactions carried out at higher temperatures and with higher ratios of ribose to **TAP** resulted in the more rapid and nearly complete modification of **TAP**, with up to 90% of all **TAP** being modified by the addition of one to three ribose molecules. This reaction was observed to happen even in aqueous solution (i.e., without drying), as **TAP**−ribose conjugates were formed in the solution state within days at temperatures from 35 to 65 °C, or weeks at 4 °C (Figures S6 and S7 SI).

Drying **TAP** with ribose results in a thick syrup with free **TAP** and **TAP**−ribose conjugates reaching a concentration of ~38% (m/m). The solubility of **TAP** in the absence of ribose is only 3.6% (m/m), indicating that a substantial fraction of **TAP** forms associations with ribose, which could include highly labile linkages between open-chain ribose and the exocyclic amines of **TAP** that may not be observed during HPLC analysis. The increased solubility of **TAP** in the presence of ribose contrasts with the relatively low solubility of the canonical nucleobases under similar conditions. For example, cytosine (the most soluble of the four RNA nucleobases) has a solubility limit in water of 0.73% (m/m), and this limit does not appear to increase with ribose as a cosolute. In addition to increasing **TAP** solubility, ribose conjugation with **TAP** could also prevent ribose degradation by fixing the sugar in its cyclized form, a possible rudimentary mechanism to aid the accumulation of ribose that is complementary to previously proposed prebiotic mechanisms, which include ribose complex formation with borate and sequestration by selective crystallization.[21−23]

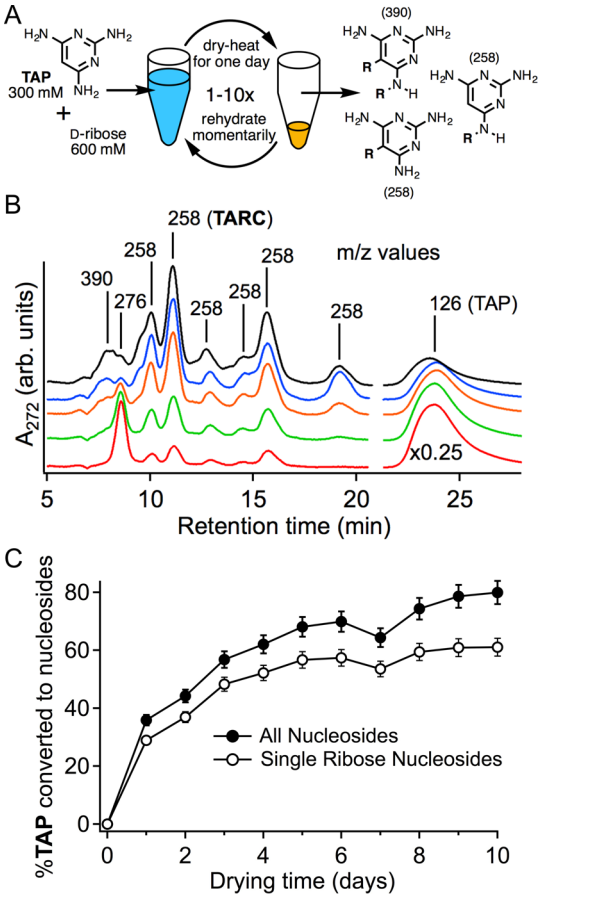

Figure 1. (A) Chemical structure of 2,4,6-triaminopyrimidine (**TAP**) and the process used to generate **TAP**-D-ribose conjugates (including nucleosides). R groups on **TAP** represent any possible ribose isomers. (B) HPLC chromatographs of samples of **TAP** and ribose after 1−5 days of drying, i.e., drying of **TAP** (300 mM) with ribose (600 mM) (pH 8) at 35 °C (vacuum assisted) with momentary rehydration every 24 h. HPLC traces, from bottom to top, correspond to reaction times of 1, 2, 3, 4, and 5 days. Peaks are labeled with m/z values obtained by simultaneous MS and UV absorption monitoring of LC. The m/z values listed correspond to **TAP** with one closed-ring ribose conjugate, 258; **TAP** with two conjugated riboses, 390; and **TAP** conjugated with an open chain ribose, 276. (C) Plot of percentage of **TAP** converted to nucleosides as a function of reaction time (same reaction conditions as in B). Error bars represent known sources of experimental uncertainty.

The Major Product of the TAP+Ribose Reaction Is a β-Ribofuranosyl *C*-Nucleoside. To confirm that nucleosides are among the products of the **TAP**+ribose reaction, the main product (~20%) resulting from the 10-day 35 °C drying reaction of a 1:2 **TAP**+ribose mixture was isolated by HPLC. NMR spectroscopy revealed that this product is 5-β-ribofuranosyl-2,4,6-triaminopyrimidine (**TARC**) (Figures 2 and S8−S10 in SI). Two-dimensional (HMBC) analysis confirmed that **TARC** is a C-nucleoside, with a C−C bond between ribose and the nucleobase (Figure 2B), while 1D ROE experiments established **TARC** to be of the β-furanose conformation (Figure 2C).

dx.doi.org/10.1021/ja410124v | J. Am. Chem. Soc. 2014, 136, 5640−5646

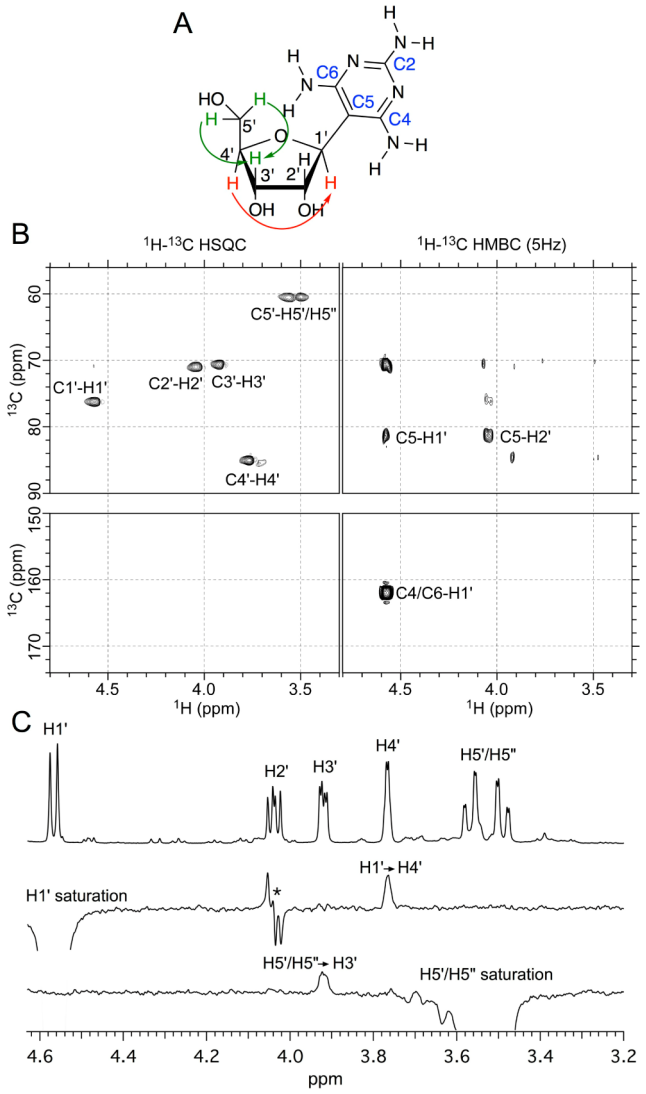

Figure 2. (A) Chemical structure of **TARC** (5-β-ribofuranose-*C*-triaminopyrimidine). Arrows show through space proton−proton magnetization transfer as indicated by ROE analysis in panel (C). (B) HMBC spectrum which was optimized for 5 Hz ^{13}C−^{1}H couplings. The ^{13}C chemical shift of 81 ppm is assigned to the C5 of the pyrimidine ring of **TARC**, and the 162 ppm chemical shift is assigned to the symmetry-related C6 and C4 carbons of the pyrimidine ring. The observed ^{1}H−^{13}C correlations between the H1′ proton and the C5 chemical shift, and the C4, C6 carbon chemical shifts, support the *C*-nucleoside structural assignment of **TARC**. (C) ^{1}H NMR and 1D ROE spectra of the nonexchangeable (ribose) protons of **TARC**. (Top) ^{1}H NMR spectrum with resonance assignments as indicated in (A). No resonances were observed in the aromatic region, consistent with the *C*-nucleoside assignment. (Middle) Irradiation of the H1′ results in through-space magnetization transfer to the H4′ proton. * indicates TOCSY transfer from H1′ to H2′, a through-bond magnetization transfer by these strongly coupled protons (e.g., 9 Hz). (Bottom) Irradiation of the H5′/H5″ protons results in through-space magnetization transfer to the H3′ proton. See SI for additional structural characterization of **TARC**.

Contemporary nucleosides are predominantly *N*-ribosides, but *C*-nucleosides do exist in nature, including pseudouridine, the most common RNA post-transcriptional nucleoside modification.[24] The finding that the ribose of **TARC** is in the β-furanose conformation, like the nucleosides found in extant life, was somewhat unexpected as free ribose exists predominantly in its β-pyranose form.[25] This discovery is consistent with previously reported model prebiotic reactions of nucleoside formation, which have also indicated that the ribofuranosyl form of nucleosides could have been available since the earliest abiotic glycosylation reactions.[9,10]

Like other 2,4,6-substituted pyrimidines, which undergo Mannich reactions,[26] **TAP** is known to be nucleophilic at the C5 position.[27] **TARC** formation is expected to proceed through the reaction of **TAP** with the free aldehyde form of ribose.[28] This proposed pathway, detailed in Figure S11 SI, is supported by the observation of a covalent intermediate in early wet−dry cycles with the mass of an open chain ribose connected to **TAP** (peak with m/z of 276 in Figure 1B and Figure S2 SI). Consistent with this putative assignment, the 276 m/z product is a transient species, appearing most prominently after the first two days of drying, but vanishing almost completely after the fifth day of drying. In contrast, **TARC** yield steadily increases up to at least 5 days of drying and does not decrease with additional drying time. It is also a certainty that exocyclic *N*-glycosides are among the **TAP**−ribose conjugates present in the crude reaction mixture, as multiple products with m/z values corresponding to **TAP** with one, two, and three covalent ribose additions are observed (which necessitates that some of these products have at least one ribose added to an exocyclic amine of **TAP**). Furthermore, formation of exocyclic *N*-glycosides involving the natural nucleobases has previously been shown to form in both drying reactions[1,2] and in solution.[29] Hydrolysis studies of the crude **TAP**−ribose reaction mixture show the rapid conversion of multiple ribose nucleosides to free **TAP** or a single ribose−**TAP** conjugate (Figure S12 SI), which is analogous to the facile release of ribose from the exocyclic amine of adenine.[1,2]

TARC Assembles with CA To Form a Hydrogel with Micrometer-Length Polymers. HPLC purified **TARC** was tested to determine if it is able to assemble with cyanuric acid (**CA**) in aqueous solution. Mixing **TARC** with **CA** in equimolar proportions in a sodium phosphate and boric acid buffer resulted in the formation of a shear-thinning hydrogel (Figure 3A). Hydrogel formation is indicative of self-assembly into supramolecular polymers that further associate to form a continuous matrix.[30]

Circular dichroism (CD) was used to inspect solutions containing **TARC** and **CA**, as dramatic changes in CD-signal intensity are often associated with the formation of supramolecular assemblies by chiral monomers.[31,32] In the present case, large, positive bands from 210 to 250 and 270−290 nm were observed for **TARC** and **CA** mixtures at 4 °C for concentrations greater than 5 mM in each monomer; a **TARC** and **CA** mixture at 2.5 mM each exhibited a CD profile essentially identical to **TARC** alone (Figure 3B and Figures S13 and S14 in SI). Heating of a sample containing 5 mM **TARC** and **CA** to 20 °C resulted in a complete loss of the assembly-induced CD signal. The **TARC** UV absorption spectrum exhibited a red-shift upon the addition of **CA**, demonstrating the formation of J-type aggregates, a spectral feature that is associated with $\pi-\pi$ stacking interactions (Figure 3C).

TARC−**CA** assemblies were visualized by atomic force microscopy (AFM), which revealed supramolecular polymers with lengths greater than 200 nm (Figure 4A). The diameter of a single fiber, measured perpendicular to the image plane, was 2 nm (inset, Figure 4A). Self-assembled structures of comparable thickness and length were recently observed when a molecule named **TAPAS** (**TAP** with succinate conjugated to an exocyclic

dx.doi.org/10.1021/ja410124v | J. Am. Chem. Soc. 2014, 136, 5640−5646

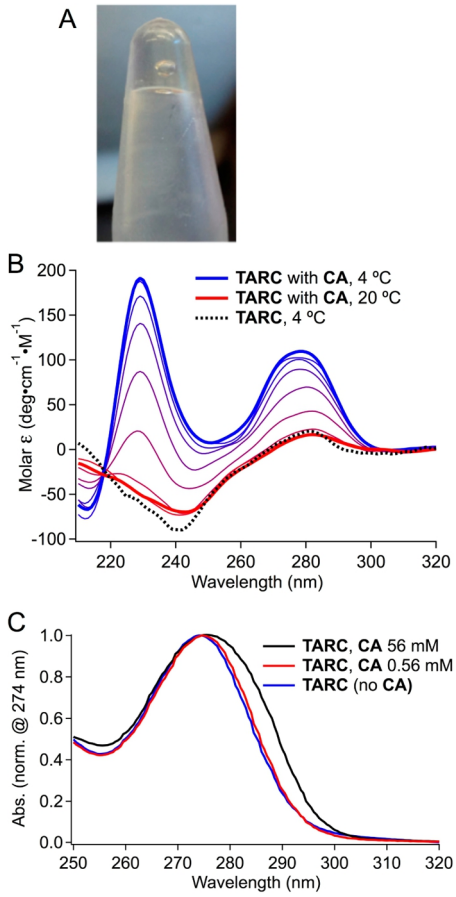

Figure 3. (A) Gel formed by **TARC** and **CA** (40 mM in each monomer). High viscosity of the gelled solution is illustrated by a bubble that remained in place indefinitely. (B) CD spectra of 5 mM **TARC** and **CA**, in 200 mM sodium phosphate/200 mM sodium borate (pH 7), at temperatures ranging from 4 to 20 °C, in steps of 2 °C. Spectrum of **TARC** in same buffer without **CA** is also shown for comparison. (C) The UV spectrum of **TARC** (56 mM) and **CA** (56 mM) at 4 °C in sodium phosphate buffer (200 mM, pH 7.0) with sodium borate (200 mM) (black), showing a red-shift characteristic of J-type aggregates when compared to **TARC** alone (blue). When the same solution was diluted by 100-fold (red), the **TARC**/**CA** UV profile matched that of **TARC** alone. All absorbances were normalized to absorbance maximum within the region shown.

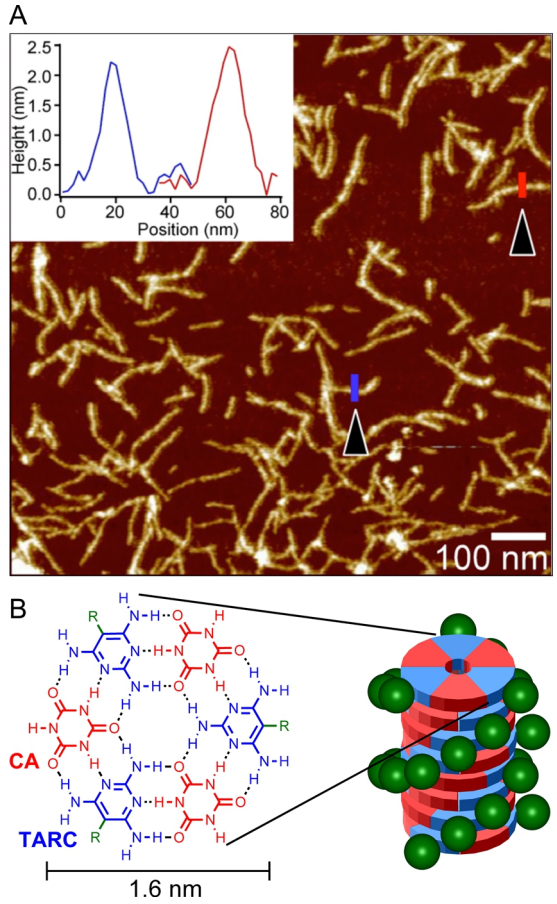

Figure 4. (A) AFM topographic image of self-assembled **TARC-CA** fibers from a solution containing 50 mM in each molecule. Inset shows the height profile of single fibers delineated by the red and blue lines in the main panel. (B) Structures of **TARC** and **CA**, in their H-bonded rosette structure, and proposed higher-order assembly based upon AFM fiber dimensions. Ribose is indicated as R on the **TARC** chemical structures and green spheres on schematic models of **TARC**. The hexad stack is depicted with a helical twist to emphasize the presence of a preferred chiral arrangement of monomers as indicated by the CD spectrum shown in Figure 3. The actual handedness and degree of helical twist has not been determined.

amine) was mixed with **CA**.[20] The similarities of these structures strongly suggest that the fibers shown in Figure 4A are **TARC** nucleosides assembled with **CA** in the same manner as **TAPAS** assembled with **CA**. That is, **CA** and **TARC** arranged within "rosettes" that are π-stacked to form linear supramolecular assemblies (Figure 4B). These assemblies have a predicted width of approximately 1.6 nm for **TAP** before conjugation with ribose, which is consistent with the measured fiber thickness of 2 nm. Given that the fibers imaged by AFM are up to 500 nm in length, and that the interplane stacking of planar ring systems is 0.34 nm, each of these linear assemblies represents up to 1500 stacked hexads.

The borate anion in the sodium borate buffer was found to be essential for the formation of water-soluble assemblies. Initial mixing experiments with **TARC** and **CA** in the absence of borate resulted in immediate precipitation, as observed when unmodified **TAP** is mixed with **CA**. The ability for borate to improve the solubility of the **TARC**−**CA** complex was not unexpected. Water-soluble rosette assemblies by **TAP** (or melamine, its triazine analogue) and **CA** have only been obtained when a charged group is incorporated at the periphery of these assemblies,[20,33] and it was anticipated that the borate anion would add a negative charge to **TARC** upon complex formation with the vicinal *cis*-diols of ribose.[22,34] With regard to the emergence of charged nucleosides (e.g., nucleotides) and their associated polymers, it is clear that phosphate is optimal for providing negative charges along the nucleic acid backbones in extant life.[35] We do not propose that borate was part of an early pre-RNA. However, other negatively charged moieties, such as gloxylate,[36] may have initially been part of a pre-RNA before being replaced by phosphate (just as there may have been different nucleoside bases in pre-RNA polymers).

TAP−Ribose Conjugates in the Crude Reaction Mixture Assemble with CA To Form Hydrogels and Micrometer-Length Fibers. In order to find a more realistic one-pot prebiotic reaction for the formation *and selection* of nucleosides, we investigated the potential of **TAP** nucleosides in the reaction mixture to associate with **CA** while still in solution with unreacted starting materials, nonpairing **TAP**−

dx.doi.org/10.1021/ja410124v | *J. Am. Chem. Soc.* 2014, 136, 5640−5646

ribose conjugates, and any other reaction products. For this investigation, the crude reaction mixture of 1 part **TAP** and 2 parts ribose that had been subjected to drying for 10 days was resuspended in sodium borate buffer, pH 8. **CA** was then added to the solution and heated to 95 °C (to facilitate dissolving **CA**). Upon cooling to room temperature the solution formed a hydrogel that coexisted with a precipitate (Figure 5A). Control

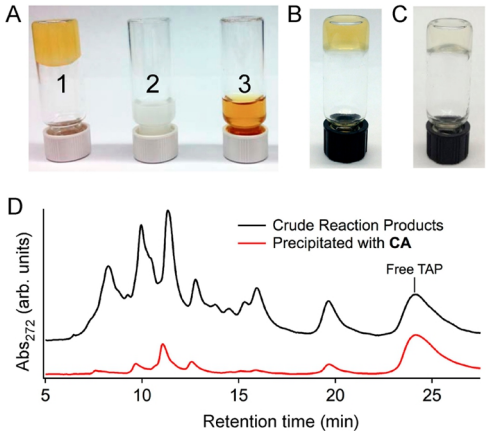

Figure 5. (A) Inverted bottle test showing gel formation of a 10-day reaction of **TAP** with ribose (1:2::**TAP**:ribose; vacuum-assisted drying at 35 °C with daily rehydration) after addition of cyanuric acid (**CA**) to the same concentration as **TAP** (modified and unmodified) (bottle 1). **CA** was added with sodium borate (300 mM, pH 8) at room temperature. Gel formation is not observed if procedure is identical to that of bottle 1, but the **TAP** and ribose solution is not subjected to drying (bottle 2), or if **CA** is not added to sample (bottle 3). (B) Same as bottle 1 in A, except **CA** was added before sample was dried to generate **TAP**–ribose conjugates. (C) Same as bottle 1 in A, except solution was clarified of precipitated material by centrifugation and diluted to 16 mM for both **CA**- and **TAP**-containing species. (D) HPLC chromatographs of the crude **TAP**+ribose reaction product used to make the gel shown in C (upper trace) and of the precipitate that formed when this crude mixture was mixed with **CA** (lower trace). Chromatographs were normalized to the integrated area of free **TAP** peaks.

experiments in which **TAP** and ribose were freshly mixed without drying, or where **CA** was not added to the postdrying **TAP**+ribose reaction mixture, did not result in hydrogel formation (Figure 5A), confirming that products of the **TAP** +ribose reaction and their assembly with **CA** are the cause of hydrogel formation. Similar hydrogels were also obtained if **CA** was initially added to an unreacted solution containing **TAP** and ribose, followed by drying and heating; confirming that the order of **CA** addition is not critical to the **TAP**+ribose reaction or hydrogel formation (Figure 5B)

The translucent hydrogel solution formed by the crude **TAP** +ribose reaction mixture and **CA** could be clarified of precipitate by centrifugation to yield a transparent hydrogel (Figure 5C). HPLC–UV analyses of the material in the gel and the precipitate revealed that the hydrogel is the preferential phase for **TAP**–ribose conjugates, whereas the precipitate is the preferential phase for unmodified **TAP** (Figure 5D). Specifically, the crude **TAP**+ribose gel contained approximately 87% of **TAP** as **TAP**–ribose conjugates and 13% as free **TAP**. In contrast, the precipitate formed upon the addition of **CA** was substantially depleted of **TAP**–ribose conjugates (43%) and enriched in free **TAP** (57%). We propose that this separation of **TAP**–ribose conjugates from free **TAP** by supramolecular polymer formation/precipitation with **CA** represents a potential prebiotic mechanism to locally concentrate pairing nucleosides away from nonpairing molecules (e.g., nonpairing **TAP**–ribose conjugates) and from precipitating molecules that do pair (e.g., free **TAP**) in a complex chemical mixture.

The hydrogel phase formed by the crude **TAP**+ribose reaction mixture and **CA** was imaged by AFM, again revealing the formation of micrometer-length fibers (Figure 6). The

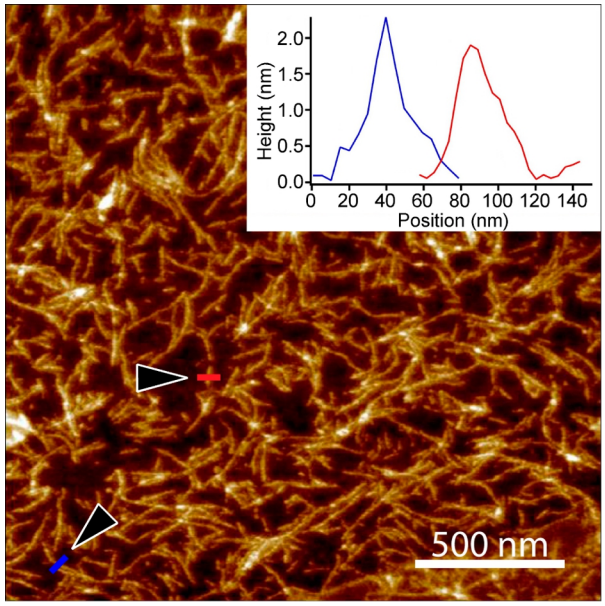

Figure 6. AFM topographical image of assemblies formed by the crude **TAP**+ribose reaction mixed with **CA** (gel shown in Figure 5C). (Inset) Height measurements across individual fibers indicated by red and blue lines and arrowheads in main image.

thickness of single fibers was determined to be 2 nm (inset, Figure 6), as found with purified **TARC** assembled with **CA**. While the **TARC**–**CA** combination is likely to be a large constituent of these noncovalent assemblies, other **TAP**–ribose conjugates may also be part of these assemblies. We are currently investigating how differences in the **TAP**–ribose conjugates, such as sugar structure and conformation, may affect their selection and inclusion into the supramolecular assemblies. Regardless, the ability of the **TAP**–ribose conjugates and **CA** to assemble into ordered supramolecular structures without the need for starting from a pure source of monomer demonstrates a robust and potentially prebiotic pathway for monomer isolation which may allow for a pathway for 'self-selection' by a stepwise constitutional preferential exclusion/inclusion mechanism.

■ CONCLUSION

In summary, we have shown that **TAP** readily forms nucleosides with ribose in a one-pot model prebiotic reaction. The high yield of the β-ribofuranoside, **TARC**, from the **TAP** +ribose reaction contrasts with the low or nonexistent nucleoside formation found in ribose reactions with the canonical nucleobases. These observations lend support to the hypothesis that there could have been alternative prebiotic nucleobases that were more amenable to spontaneous nucleoside formation.[14,37,38] Furthermore, the addition of a complementary H-bonding heterocycle with **TAP** nucleosides, even in the crude **TAP**+ribose reaction mixture, results in the

dx.doi.org/10.1021/ja410124v | *J. Am. Chem. Soc.* 2014, 136, 5640–5646

self-assembly of micrometer-length noncovalent polymers. Spatial ordering and increased local concentration of monomers is critical for efficient polymerization, and among the principal mechanisms by which enzymes (including polymerases) catalyze bimolecular reactions. Because highly evolved enzymes would not have existed at the origin of biopolymers (or at the origin of ancestral biopolymers), it has long been speculated that mineral surfaces[39,40] or small, organic molecules[41] may have played an important role in locally concentrating and organizing monomers prior to polymerization. Likewise, self-assembling nucleosides, like **TARC** and **CA**, would facilitate monomer coupling (with appropriate ligation chemistry) and thereby the *de novo* formation of covalent, proto-biopolymers. In this context, the results presented begin to address how alternative nucleobases that readily self-assemble could have set the stage for the emergence of the early informational polymers of life by both facilitating nucleoside formation and the selection of pairing bases from complex mixtures, before the emergence of enzymes.

METHODS

Drying−Heating Reactions of TAP with Ribose. Stock solutions of 2,4,6-triaminopyrimidine (Acros Organic) and D-ribose (Amresco and Sigma-Aldrich) were prepared in nanopure H_2O. When dried at 45−95 °C, an Eppendorf tube with 1 mL of the stock solution was placed in a dry block heater at the specified temperature. For drying at 35 °C, tubes were placed in a vacuum centrifuge. Samples that were reacted for multiple days were dried for 24 h, the resultant highly viscous solution was momentarily resuspended in the original volume of nanopure H_2O, and the process was repeated for the indicated number of days. Momentary hydration was performed to ensure that the solution was homogeneous during the course of the reaction. Additionally, daily hydration of the reaction mixtures models environmental day/night cycles, a process which would have been operative on the prebiotic Earth. Analytical HPLC of samples was performed by running 95% 0.010 M NH_4HCO_3 (pH 7.2) and 5% CH_3OH at 0.5 mL·min^{-1} through a Phenomenex Synergi Polar-RP 80 Å column (250 mm × 4.60 mm × 4 μm).

Preparative Synthesis of 5-β-Ribofuranosyl-2,4,6-triaminopyrimidine. 2,4,6-Triaminopyrimidine (1.5 mmol) and D-ribose (3 mmol/2 equiv) were dissolved in 5 mL of nanopure H_2O. The sample was subjected to drying in a vacuum centrifuge for one week. The resulting light-brown, highly viscous crude mixture was resuspended in 2.5 mL of 50 mM CH_3COONa buffer at pH 4.6. The solution was then loaded onto a gravity column containing Sephadex C50 sulfopropyl cation-exchange media, and was eluted with a gradient of CH_3COONH_4 in 50 mM CH_3COONa buffer at pH 4.6. The resultant product-containing fractions were concentrated under vacuum to remove water. **TARC** was purified using an Agilent 1200 Infinity system by ion-pairing chromatography on a semipreparative Phenomenex Prodigy ODS(3) 100 Å column (250 mm × 10 mm × 5 μm), with a mobile phase of 100% 0.1 M triethylammonium acetate. The resultant product-containing fractions were concentrated under vacuum, removing the majority of volatile salts from the various purification steps. Additional desalting was accomplished by reverse phase chromatography on the previously mentioned semipreparative column. Maximum yield of **TARC** obtained was 20%. UV/vis (H_2O, pH 7): λ_{max} = 276 nm ε_{276} = 13,600 mol·L^{-1}·cm^{-1}. ^{1}H NMR (500 MHz, D_2O) δ 4.57 (d, 9.1 Hz, H1′); 4.04 (dd, 9.1, 6.2 Hz, H2′); 3.92 (dd, 2.6, 6.2 Hz, H3′); 3.77 (m, 2.5 Hz, H4′); 3.57 (m, ABX, 2.0, 12.5 Hz, H5′a); 3.49 (m, ABX, 2.4, 12.6 Hz, H5′b). ^{13}C NMR (126 MHz, D_2O) δ 161.93 (C4/C6); 160.6 (C2); 84.9 (C4′); 76.2 (C1′); 81.3 (C5); 70.9 (C2′); 70.6 (C3′); 60.4 (C5′). HRMS (pos. m/z): $C_9H_{16}O_4N_5$ theoretical mass: 258.1197, actual mass: 258.1199.

Crude and TARC Gel Preparation. The crude gel was formed by combining **CA** (1.5 mmol/1 equiv) with the 10-day dried **TAP** + ribose reaction product (see Preparative Synthesis above) and then dissolved in 300 mM sodium borate (pH 8) to reconstitute the sample at 5 mL. Reactions containing **CA** were carried out the same as with the **TAP** + ribose reactions except one equivalent of **CA** was included with the starting material. In all cases the samples were then heated to 95 °C for 5 min to dissolve the **CA** and cooled at room temperature. A cloudy, yellow hydrogel was observed with an off-white precipitate collected at the bottom. Samples from the original crude reaction, precipitate, and hydrogel were collected and analyzed by HPLC-DAD. Co-injection and LC−MS analysis were used to identify **TAP** from **TAP**−ribose conjugates. Clarified hydrogels were obtained by centrifugation of the crude gel through a 0.2 μm Millipore spin column. Gels prepared with purified **TARC** were made by the same procedure with the addition of 200 mM sodium phosphate to buffer at pH 7.

Analytical Techniques. CD spectra were obtained on a Jasco J-720 CD spectrometer, and acquired by scanning 200−350 nm at a rate of 500 nm/min, with averaging of 20 measurements. UV absorption analysis was performed on an Agilent 8453 UV−vis spectrophotometer equipped with an 89090A temperature controller. All samples that were inspected by CD or UV contained 200 mM sodium phosphate and 200 mM boric acid (pH 7) and were analyzed in a torsion-free sandwich cell with either a 0.1 or 0.01 mm path length. The structure of **TARC** was then confirmed by NMR using ^{1}H NMR, ^{13}C NMR, COSY, HSQC, HMBC, and ROE, all collected on a Bruker DRX-500. High-resolution mass spectrometry was performed on a Waters Synapt G2; purity was confirmed by analytical HPLC as described in the analytical synthesis of **TARC**.

AFM Imaging. Samples were imaged by AFM over a silicon surface. Prior to deposition, silicon wafers were rinsed with nanopure water followed by ethanol and dried under a N_2 stream. After rinsing, silicon surfaces were cleaned with UV-ozone for 30 min (JE- LIGHT UVO Cleaner model #42) and stored in a Petri dish until use. A 1.5-μL sample that was stored on ice was spin coated (Laurell Technologies) at 4 °C for 30 s (2000 rpm, Figure 2C; 4000 rpm, Figure 3D). After spin coating, the sample was dried at room temperature in a Petri dish overnight. The AFM imaging was performed on a Multimode AFM with Nanoscope IIIa controller and a "J" scanner (Veeco Instruments) in tapping mode in air, using Si tips (Vistaprobes, 40 N/m).

ASSOCIATED CONTENT

Supporting Information

Additional characterization of the formation of **TARC** is given in Figures S1−S7 and S12, detailed NMR characterization of **TARC** is given in Figures S8−S10, a proposed reaction mechanism for the formation of **TARC** from **TAP** and ribose is presented in Figure S11. Additional CD characterization of **TARC** assemblies is given in Figures S13−S14. This material is available free of charge via the Internet at http://pubs.acs.org.

AUTHOR INFORMATION

Corresponding Author

hud@gatech.edu

Author Contributions

‡M.C.C. and B.J.C. contributed equally to this work

Notes

The authors declare no competing financial interest.

ACKNOWLEDGMENTS

This work was jointly supported by the NSF and the NASA Astrobiology Program, under the NSF Center for Chemical Evolution, CHE-1004570 (N.V.H., M.C.C., I.M., I.G., J.K., R.K.), and the NASA Exobiology Program NNX13AI02G (N.V.H., M.C.C., B.J.C.). We thank L. A. Bottomley for use of AFM, F. A. L. Anet, A. E. Engelhart, L. D. Williams, and G. B. Schuster for discussions.

REFERENCES

(1) Fuller, W. D.; Sanchez, R. A.; Orgel, L. E. *J. Mol. Biol.* **1972**, *67*, 25−33.
(2) Fuller, W. D.; Sanchez, R. A.; Orgel, L. E. *J. Mol. Evol.* **1972**, *1*, 249−257.
(3) Maurel, M.-C.; Convert, O. *Origins Life Evol. B* **1990**, *20*, 43−48.
(4) Sanchez, R. A.; Orgel, L. E. *J. Mol. Biol.* **1970**, *47*, 531−543.
(5) Powner, M. W.; Gerland, B.; Sutherland, J. D. *Nature* **2009**, *459*, 239−242.
(6) Powner, M. W.; Sutherland, J. D.; Szostak, J. W. *Synlett* **2011**, 1956−1964.
(7) Joyce, G. F.; Schwartz, A. W.; Miller, S. L.; Orgel, L. E. *Proc. Natl. Acad. Sci. U.S.A.* **1987**, *84*, 4398−402.
(8) Orgel, L. E. *Crit. Rev. Biochem. Mol. Biol.* **2004**, *39*, 99−123.
(9) Kolb, V. M.; Dworkin, J. P.; Miller, S. L. *J. Mol. Evol.* **1994**, *38*, 549−557.
(10) Bean, H. D.; Sheng, Y. H.; Collins, J. P.; Anet, F. A. L.; Leszczynski, J.; Hud, N. V. *J. Am. Chem. Soc.* **2007**, *129*, 9556−9557.
(11) Solie, T. N.; Schellman, J. A. *J. Mol. Biol.* **1968**, *33*, 61−77.
(12) Ts'o, P.; Melvin, I.; Olson, A. *J. Am. Chem. Soc.* **1963**, *85*, 1289−1296.
(13) Engelhart, A. E.; Hud, N. V. *Cold Spring Harbor Perspect. Biol.* 2010, *2*, 10.1101/cshperspect.a002196.
(14) Hud, N. V.; Cafferty, B. J.; Krishnamurthy, R.; Williams, L. D. *Chem. Biol.* **2013**, *20*, 466−474.
(15) Rembold, H.; Schramm, H. J. *Chem.Ber.* **1963**, *96*, 2786−2797.
(16) Lehn, J. M.; Mascal, M.; Decian, A.; Fischer, J. *J. Chem. Soc., Perkin Trans. 2* **1992**, 461−467.
(17) Bohanon, T. M.; Denzinger, S.; Fink, R.; Paulus, W.; Ringsdorf, H.; Weck, M. *Angew. Chem., Int. Ed. Engl.* **1995**, *34*, 58−60.
(18) Marchi-Artzner, V.; Artzner, F.; Karthaus, O.; Shimomura, M.; Ariga, K.; Kunitake, T.; Lehn, J. M. *Langmuir* **1998**, *14*, 5164−5171.
(19) Rakotondradany, F.; Palmer, A.; Toader, V.; Chen, B. Z.; Whitehead, M. A.; Sleiman, H. F. *Chem. Commun.* **2005**, 5441−5443.
(20) Cafferty, B. J.; Gállego, I.; Chen, M. C.; Farley, K. I.; Eritja, R.; Hud, N. V. *J. Am. Chem. Soc.* **2013**, *135*, 2447−2450.
(21) Prieur, B. E. *C.R. Acad. Sci. Paris, Chim./Chem.* **2001**, *4*, 667−670.
(22) Ricardo, A.; Carrigan, M. A.; Olcott, A. N.; Benner, S. A. *Science* **2004**, *303*, 196−196.
(23) Springsteen, G.; Joyce, G. F. *J. Am. Chem. Soc.* **2004**, *126*, 9578−9583.
(24) Charette, M.; Gray, M. W. *IUBMB Life* **2000**, *49*, 341−351.
(25) Angyal, S.; Pickles, V. *Aust. J. Chem.* **1972**, *25*, 1695−1710.
(26) Han, B.; Rajwanshi, V.; Nandy, J.; Krishnamurthy, R.; Eschenmoser, A. *Synlett* **2005**, *16*, 0744−0750.
(27) Delia, T. J.; Kirt, D. D.; Sami, S. M. *J. Heterocycl. Chem.* **1983**, *20*, 145−147.
(28) Dworkin, J. P.; Miller, S. L. *Carbohydr. Res.* **2000**, *39*, 359−365.
(29) Johnson, K. M.; Price, N. E.; Wang, J.; Fekry, M. I.; Dutta, S.; Seiner, D. R.; Wang, Y.; Gates, K. S. *J. Am. Chem. Soc.* **2012**, *135*, 1015−1025.
(30) Estoff, L. A. H.; A, D. *Chem. Rev.* **2004**, *104*, 1201−1217.
(31) Fenniri, H.; Packiarajan, M.; Vidale, K. L.; Sherman, D. M.; Hallenga, K.; Wood, K. V.; Stowell, J. G. *J. Am. Chem. Soc.* **2001**, *123*, 3854−3855.
(32) Hirschberg, J. H. K. K.; Brunsveld, L.; Ramzi, A.; Vekemans, J. A. J. M.; Sijbesma, R. P.; Meijer, E. W. *Nature* **2000**, *407*, 167−170.
(33) Ma, M. M.; Bong, D. *Langmuir* **2011**, *27*, 8841−8853.
(34) Springsteen, G.; Wang, B. *Tetrahedron* **2002**, *58*, 5291−5300.
(35) Westheimer, F. H. *Science* **1987**, *235*, 1173−1178.
(36) Bean, H. D.; Anet, F. A. L.; Gould, I. R.; Hud, N. V. *Orig. Life Evol. B* **2006**, *36*, 39−63.
(37) Rios, A. C.; Tor, Y. *Astrobiology* **2012**, *12*, 884−891.
(38) Rios, A. C.; Tor, Y. *Isr. J. Chem.* **2013**, *53*, 469−483.
(39) Bernal, J. D. *The Physical Basis of Life*; Routledge & Kegan Paul: London, 1951.
(40) Ferris, J. P.; Aubrey R. Hill, J.; Liu, R.; Orgel, L. E. *Nature* **1996**, *381*, 59−61.
(41) Jain, S. S.; Anet, F. A. L.; Stahle, C. J.; Hud, N. V. *Angew. Chem., Int. Ed.* **2004**, *43*, 2004−2008.